JOURNAL OF SPACECRAFT AND ROCKETS
Vol. 40, No. 1, January–February 2003

Ground Demonstration of a Spinning Solar Sail Deployment Concept

M. Salama,* C. White,† and R. Leland‡
Jet Propulsion Laboratory, California Institute of Technology, Pasadena, California 91109

We describe laboratory experiments to investigate the dynamics of spin deployment of a solar sail concept, originally intended for the Interstellar Probe Mission. The spin-deployment concept is first described. A series of three experiments with increasing degrees of complexity were designed and performed and culminated in spin deploying a small-scale solar sail 2.5-μm-thin Mylar® film, 80 cm in diameter. The objectives were to explore the feasibility of the deployment concept and any related handling issues and to discover/understand possible modes of instability. To gain insight into the practicality of the deployment scheme, a tether configuration emulating the sail film was first deployed successfully in air and gravity. A 120-μm nylon film was then used for the sail deployment experiment, also in air and gravity. These two initial experiments were particularly useful for refining the experimental setup and handling procedures. Even though the influence of air drag and gravity was apparent, both of these experiments deployed without entanglements. With the exception of some handling issues, the ultrathin 2.5-μm Mylar film was successfully deployed in vacuum without entanglement. Design details and observations of these experiments are discussed. An approach to model numerically the spin-deployment dynamics is also described, and the results of simulating the dynamics of tether deployment are given.

Nomenclature

t_r	=	time for release of radial restraint, s
Δt	=	maximum ramp-up time, s
$\omega_{\max}$	=	maximum angular velocity, cycles/s
$\omega_0(t)$	=	time-dependent angular velocity for spinning the central hub, cycles/s

Introduction

SINCE the early 20th century, solar sailing has been advocated as an efficient means of space propulsion. Although a solar sail has yet to be flown, the practicality of the concept has been confirmed by numerous recent studies.[1,2] Several solar sail design options have been considered in depth for a wide variety of space travel, ranging from Earth orbiting to interstellar. Two primary solar sail design concepts have emerged: three-axis-stabilized square sails and spin-stabilized sails. In the first, lightweight compressive booms emanating from a central hub form the primary load-carrying structural members. The compressive loads in the booms result from tensioning the sail film. In the second, the dynamics of spinning induce the needed tension field in the sail, thereby providing the desired near flatness of the film. Within these two options, there are still several other distinct concepts, each having its own set of merits and challenges. In all cases, however, the solar sail must be made of large areas (several hundreds of square meters) of ultralight, highly reflective thin film (orders of micrometers) that can be packaged into small volume during launch, then deployed to their full gossamer proportions once on-orbit. The viability of such a technology is replete with practical questions and uncertainties that must be first examined by analysis, laboratory experiments, and flight tests, before actual flight. To this end, two significant developments have taken place during the past decade.

Received 12 June 2001; revision received 11 February 2002; accepted for publication 13 February 2002.

*Principal Engineer, Mechanical Systems Engineering and Research. Associate Fellow AIAA.
†Senior Engineer, Mechanical Systems Engineering and Research. Member AIAA.
‡Senior Technical Assistant, Mechanical Systems Engineering and Research.

First, in the early 1990s Russian investigators began a reflector technology development program that culminated in the space deployment in 1993 of a 20-m-diam spinning reflector, known as the Znamya-2 experiment.[3] As the ground development program progressed, close interaction between theoretical work and experimental experience proved to be indispensable and eventually led to the success of the in-space experiment. Second, in support of a proposed three-axis-stabilized sailcraft concept intended for use in a geostationary orbit, a ground-test program[4] was conducted in 1999 by DLR, German Aerospace Research Center/ESA in collaboration with the Jet Propulsion Laboratory (JPL)/NASA. The program intended to show the feasibility of manufacturing a 20×20 m square sail using deployable lightweight booms and extremely thin sail. Functionality of deployment of the collapsible composite boom and the ability to handle extremely thin sail film (4.0-μm PEN film) were demonstrated in simulated zero-gravity and ambient environmental conditions.

For spinning sailcrafts, the dynamics of sail deployment is perhaps one of the most challenging elements of their design. During deployment, the sail mass (which could easily amount to 50% of the total sailcraft mass) must undergo extreme dynamic transformations from the compact packaging to the fully deployed gossamer configuration. Thus, a stable and controllable deployment must be assured. Herein, the paper will focus on a preliminary design implementation, analysis simulation, and demonstration of a laboratory experiment dedicated to examining the deployment dynamics and stability of a subscale 80-cm-diam spinning sail. The work is intended as a subscale validation of a spinning sail deployment concept proposed for a NASA interstellar mission.

Spinning Sail Concept

The spinning sail concept under consideration was developed as part of a recent study to send a scientific probe to the heliopause and beyond.[5] The basic sail configuration for this mission (referred to as the Interstellar Probe Mission) is shown in Fig. 1. It consists of six sectors, which comprise a nearly 400-m-diam, less than 1-μm thin sail. Each sector is tethered to its contiguous neighbors at the perimeter and is initially stowed into Z-folded gores wrapped around a central cylindrical hub. Initial spin-up is accomplished by first deploying three 10-m-long booms to which cold gas thrusters are mounted. Once a steady spinning rate is achieved, the sail gores are released from the hub. The centrifugal acceleration then gradually unfurls the sail gores from the star shape to the ring shape with tethers attaching the sail membrane to the central hub. Pulling on

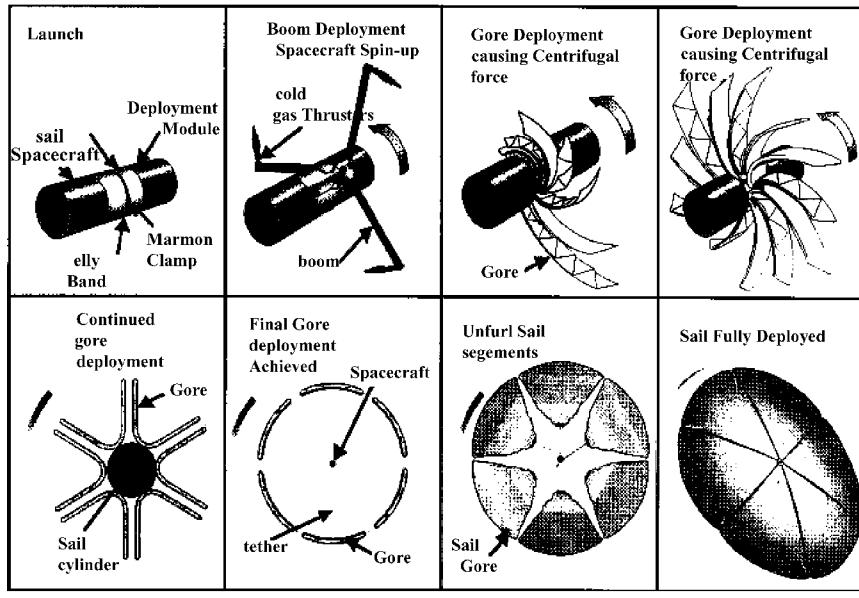

Fig. 1 Deployment concept for the Interstellar Probe Mission.

the tethers will then complete deployment of the entire 400-m-diam sail.

With the basic deployment sequence retained, the following laboratory experiments are intended to explore the feasibility of the concept, with emphasis on the dynamics and stability of the deployment process. The two main differences between the Interstellar Probe deployment concept and the deployment scheme used in the experiment are that 1) spinning is initiated by motors rather than by cold-gas thrusters and that 2) the gores are made to deploy directly from the star shape to the sector shape, without having to go through the intermediate ring configuration.

Laboratory Experiments

With reference to Fig. 1, it was envisioned that the most challenging part of the deployment would be the four steps in the lower row, which include the transformation from the star configuration to the ring configuration with the sail Z folded, followed by unrolling of the sail by pulling on the radial tethers. Within this sequence of steps, there naturally arose questions of the influence of gravity, air drag, rotation rate, radial tether release rate, and sensitivities to random small asymmetries in the experimental apparatus. To isolate and control these variables as much as possible, the deployment sequence was broken into three smaller experiments, each one increasing in complexity and culminating in the deployment of a disk-shaped sail of 2.5-μm thin film.

The first experiment used a continuous ring-shaped tether in place of the Z-folded sail membrane to demonstrate the radial release from the star configuration to the ring configuration. For the second experiment, a relatively thick 120-μm nylon film was used that was Z folded for stowage and reinforced along the perimeter with the tether. The third experiment used a rather delicate 2.5-μm aluminized Mylar® film material, Z folded with no perimeter tether reinforcement.

All three experiments used the same hardware apparatus, shown in Fig. 2. The spinning central hub consisted of two concentric, thin-walled cylindrical drums of fiberglass–fabric laminate (grade G-10), each controlled by an electric motor. The inner cylinder (5-cm diam) serves as the drum for stowing and controlling the radial tethers. The outer cylinder, or spool (10-cm diam), provides for the attachments of the sail film. As shown in Fig. 2, the motor controlling the inner drum is mounted on the base plate of the outer spool and made to rotate with it. Power is communicated to this motor through a slip ring assembly. The inner drum is then made to rotate very slowly with respect to the outer spool, thus allowing radial deployment and retraction of the tethers, which pass through small holes in the outer spool wall. A sail diameter of

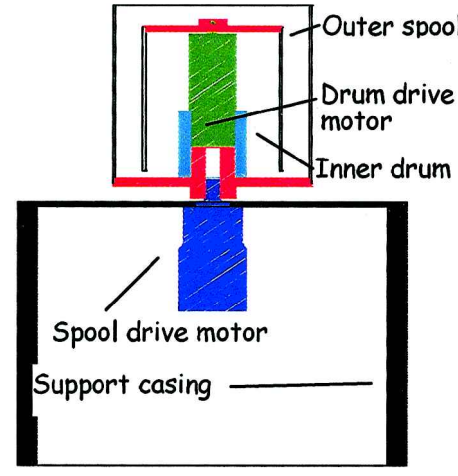

Fig. 2 Schematic of spin deployment apparatus.

80 cm was selected based on the diameter of the available vacuum chamber, 90 cm.

Experiment 1: Tether Deployment

As mentioned, the purpose of deploying a tether from the star to ring configuration was to demonstrate one of the essential deployment maneuvers using a simplified experiment that minimizes the difficulties of handling the very fragile Mylar film material. In selecting the tether material, care was taken to use rope of a reasonable mass and a sufficiently low bending stiffness. The rope tether used in the experiment had a mass of 5.5 g. Radial tethers were selected with sufficiently low mass and surface smoothness. The six radial tethers were precisely marked and cut to the same length before being attached to the central drum and fed through the holes in the outer spool. The free ends were then glued with cyanoacrylate to the ring-shaped tether at 60-deg intervals.

Spin-up and deployment to the ring configuration were accomplished on the first attempt without any difficulties. Retraction back to the star configuration was also successful. Still photographs of the steady-state configuration are shown in Figs. 3 and 4. Gravitational forces caused the tether to deflect down from the horizontal plane, but it was observed that rotational rates of approximately 200 rpm would essentially cancel these deflections.

The effect of air drag (on both the rope tether and the radial release tethers) was evident; even at steady state, the radial tethers did not

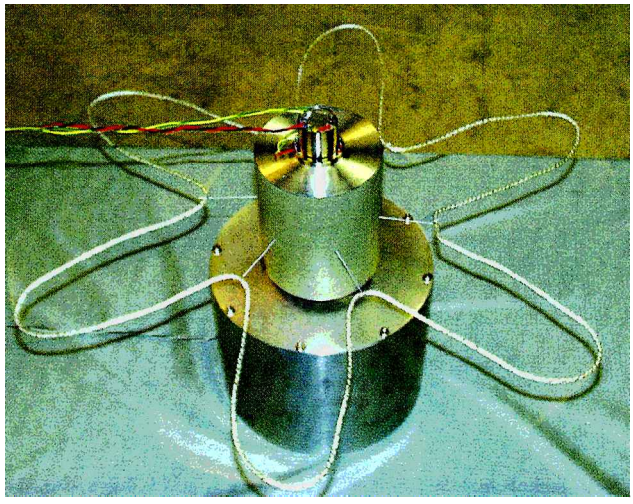

Fig. 3 Partially deployed tether.

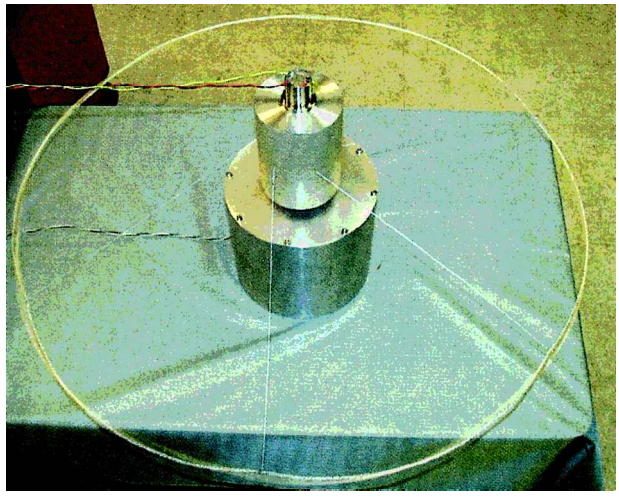

Fig. 4 Fully deployed tether.

emanate from the spool along radial lines, but rather lagged behind the spool by as much as 45 deg. Although gravity and air drag did affect the dynamics of the tethers, the experiment was nevertheless successful at demonstrating the viability of the deployment concept, as well as evaluating the experimental apparatus itself. Because the primary interest of the experiment was demonstrating the spin deployment of the thin-film structure, the tether dynamics was studied further analytically rather than experimentally.

Experiments 2 and 3: Film Deployment

Nylon Film Deployment

This set of experiments presented the practical challenges of working with stowed and deployed thin-film structures. Experimenting first with the 120-μm nylon film, however, eliminated a few of the harder challenges, while still providing experience that would be valuable for the fragile 2.5-μm Mylar film. The greatest benefit of the nylon lies not so much in its greater thickness but in its relative toughness and tear resistance.

It was decided to divide the disk-shaped sail into six 60-deg sectors. These sectors were formed by cutting a disk-shaped blank of material along radial lines from the center to outside edge, leaving a 2-cm strip of continuous material along the outside edge. This strip was then folded over the perimeter tether and sewn, thereby encasing the tether. The intention was to use the tether mass to provide extra centrifugal force to ensure full film deployment and nearly flat spinning sail. However, sewing the film created undesirable bunching up of the nylon and introduced local film wrinkling and stiffening.

A Z-fold pattern with fold lines spaced approximately 3 cm apart was chosen for folding and stowing each sector. The 3-cm spacing gave about 13 folds per sector. To accommodate the radial tethers, holes were punched through the film, midway between each fold line. The inside edge of the sail was simply taped to the outer spool, and the radial tethers were fed through the holes in the film, then glued to the perimeter tether. The final step of the installation process required simultaneously folding all six sectors and retracting the radial tethers to arrive ultimately at the star configuration.

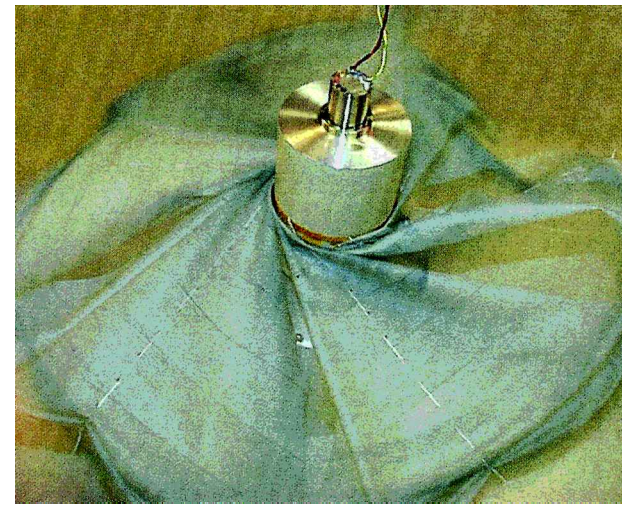

Fig. 5 Initial attempt to deploy 120-μm film.

When started from the star configuration, initial spin-up and deployment of the nylon film was attempted on the bench top, but it was immediately clear that air drag would be far too great. Figure 5 captures this initial attempt in a still photograph. It can be seen that in-plane shear stresses in the film (resulting from air drag) are causing the film to wrinkle and wind itself around the spool.

The experiment was then moved to the vacuum chamber, and the atmosphere was evacuated to a pressure of approximately 10 Pa. Inside the vacuum chamber, the sail deployment was successful, although it was not possible to make clear photographs of this first attempt. Subsequent deployments without the perimeter tether were also successful, and it was concluded that the circumferential tether was not necessary. Successful deployments using estimated rotation rates as low as 100 rpm were observed, but no attempt was made to determine a minimum rate. In none of the tests did any of the sectors bind, fail to deploy, or become entangled.

Mylar Film Deployment

A 2.5-μm-aluminized Mylar film reinforced with Kapton® threads running in one direction was used in this test. This material had an areal density of approximately 5.1 g/m^2, and an extremely low resistance to tearing, although the reinforcing did help somewhat. Because of the rather narrow dimensions of the bulk Mylar film, each of the six sectors had to be cut from the sheet separately, so that a continuous circumferential strip (if it was to be used) would have to be fabricated by adhesion. Therefore, it was decided to try six independent sectors with no circumferential connections between them.

After the sectors were cut, holes were punched between each of the 13 fold lines. The sectors were carefully taped to the outer spool as before, and the radial tethers were fed through the holes. The free ends of the tethers were taped with small pieces of tape to the outer edge of the sectors. Because the sectors were independent, it was possible in this case to Z fold each one separately, while manually controlling the radial tether by gently pulling it through the wall of the outer spool from the inside. The installation was complete once the star configuration was achieved. Details of the spool attachment are shown in Fig. 6.

Deploying the 2.5-μm Mylar film under 10-Pa vacuum was not the immediate success that it had been with the tether and with the nylon film. When started from rest, the rotational speed was slowly increased to approximately 200 rpm. The radial tethers were then activated for release, but the sail did not deploy. In an attempt to force deployment of the sail, the rotational speed was increased further, and the radial motor was switched on/off numerous times.

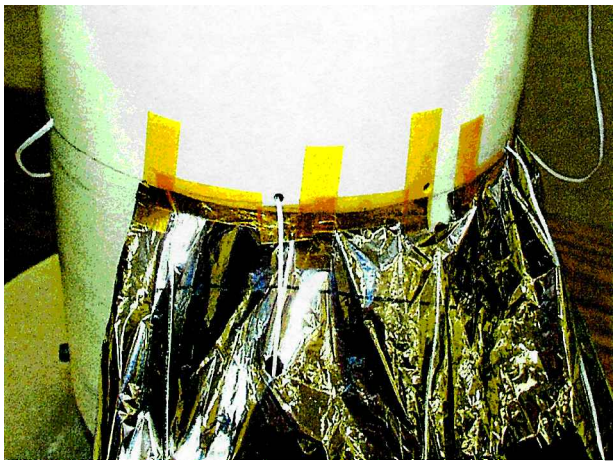

Fig. 6 Film attachment to the hub.

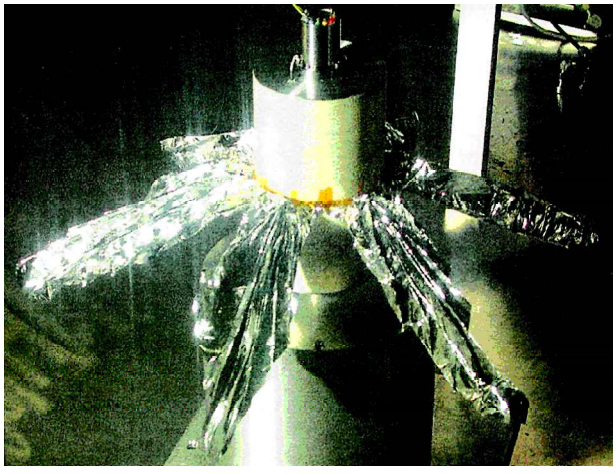

Fig. 7 Sail film before radial deployment.

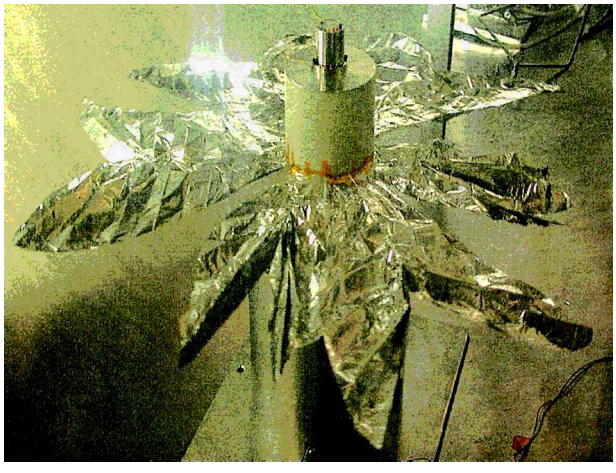

Fig. 8 Partial deployment with binding film.

Suddenly, the sail deployed to near its full configuration. Subsequently, as the radial tethers were fully extended, the sail fully deployed. Figures 7–10 show a sequence of photographs that were taken at various stages in the deployment process from the view port in the vacuum chamber. The leading causes for the tardy deployment are most likely due to binding or unintended sticking within the folds of the sectors due to small areas of exposed tape adhesive. In fact, one of the lessons learned from working with the metalized Mylar film is to avoid the use of tape whenever possible. Postdeployment inspection of the sail revealed tearing up to 2 cm in length in two of the six sectors, particularly near the inside edge

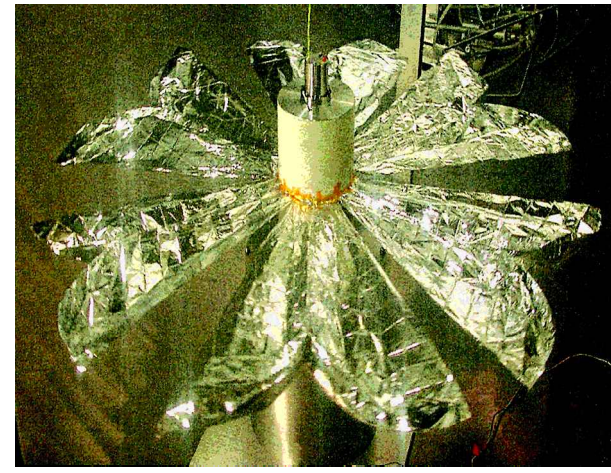

Fig. 9 Partial deployment, sector extended.

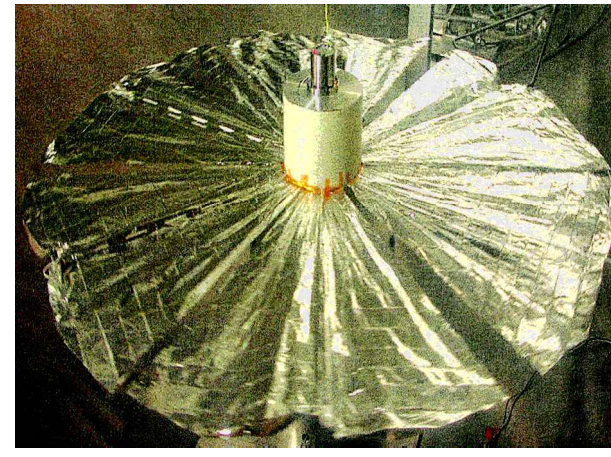

Fig. 10 Fully deployed 2.5-μm film.

of the sail in the vicinity of the first radial-tether hole and at the last hole near the outside edge of the sail.

Numerical Simulations of Tether Deployment

The dynamics of tether deployment was analyzed using DYNA3D. The tether deployment analysis was intended as a first step toward modeling the film deployment. The gravitational field and air drag were not modeled. Characteristics of the tether were chosen to match the experiment. This includes length, mass per unit length, and modulus. Rather than six tether sectors, only four, each covering a 90-deg sector were assumed, and each was modeled with 55 elements having only uniaxial stiffness, area equal to $1.0e{-}5$ m^2 and modulus equal to $1.0e{+}9$ N/m^2. Initially, each of the four tethers was attached to the rigid cylinder at two points and then wrapped around as shown in Fig 11. At $t = 0$, no contact or elastic interaction was assumed between the tethers and/or the rigid cylinder.

Deployment was accomplished in two stages, the interaction of which could be a design parameter to be selected. First was the spin-up and ensuing transient response of the tethers to the induced rotation. Spin-up was accomplished by prescribing the angular velocity $\omega_0(t)$ of the central rigid cylinder such that

$$\omega_0(t) = \begin{cases} t \cdot (\omega_{\max}/\Delta t), & 0 \le t < \Delta t \\ \omega_{\max}, & t \ge \Delta t \end{cases} \tag{1}$$

where $\omega_{\max} = 4$ cycles/s and Δt is a ramp-up time selected parametrically from 0.01 to 2.0 s. At a prescribed time, $t_r \ge \Delta t$, in presence of the spin-up acceleration field, the second stage of deployment was initiated by simultaneously releasing all four tethers at a prescribed rate relative to their attachment points on the rigid cylinder. Because of the centrifugal accelerations, the tethers will tend to move radially outward.

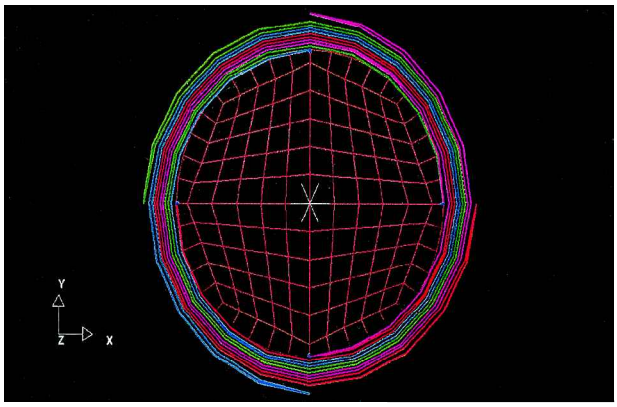

Fig. 11 Model of four stowed tether segments.

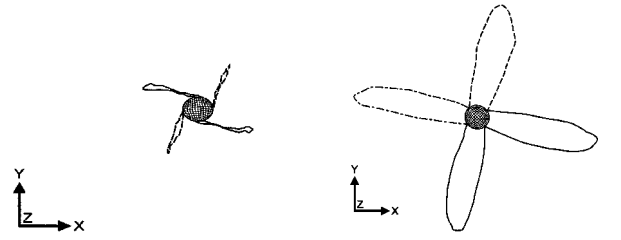

a) Step 4, time = 1.1999798*e*−01 d) Step 41, time = 1.5999978*e*+00

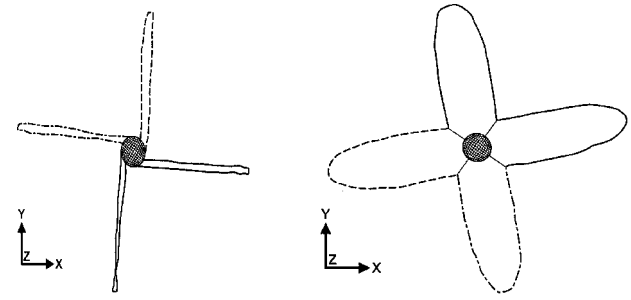

b) Step 11, time = 3.9999810*e*−01 e) Step 58, time = 2.2799950*e*+00

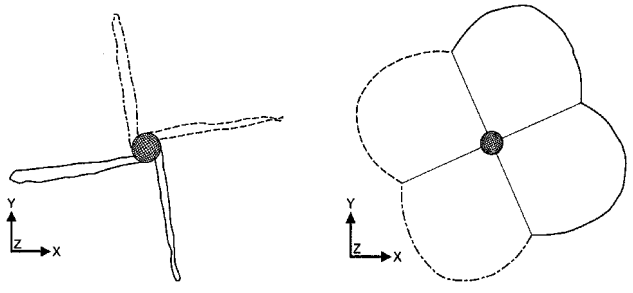

c) Step 16, time = 5.9999788*e*−01 f) Step 90, time = 3.5599959*e*+00

Fig. 12 Simulation of tether deployment (nominal case).

In addition to these initial and intermediate enforced motions, the tethers were also subjected to their own material damping, as well as to contact forces arising from possible interactions among each other and with the rigid cylinder. A nominal mass-proportional damping of 5% critical was assumed equally for each tether, but was later varied.

Contact interactions were also modeled. During a time step, if a node on the tether is within a small distance ε_n from the rigid cylindrical surface, and the relative velocity between them is negative, that is, contact closure, the tether node is constrained to move consistently with the rigid cylinder surface. The constraint is relaxed if in a subsequent step the updated nodal relative velocity indicates contact separation. On the other hand, contact between the tethers was implemented as a special case of the surface-to-surface contact,[6] where equal and opposite contact forces are applied to

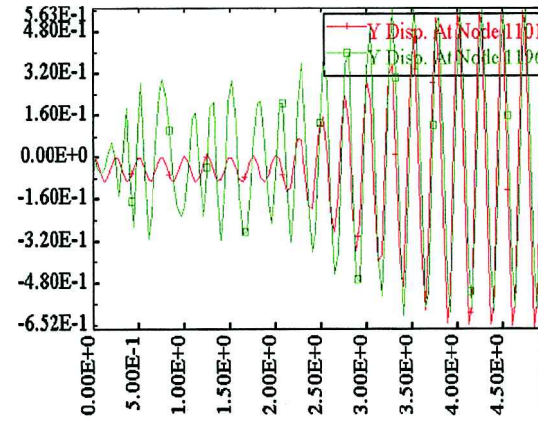

Fig. 13a Fast spin-up, $\Delta t = 0.01$ s.

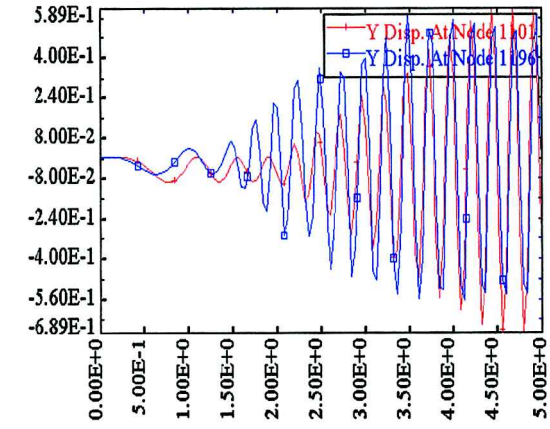

Fig. 13b Slow spin-up, $\Delta t = 2.0$ s.

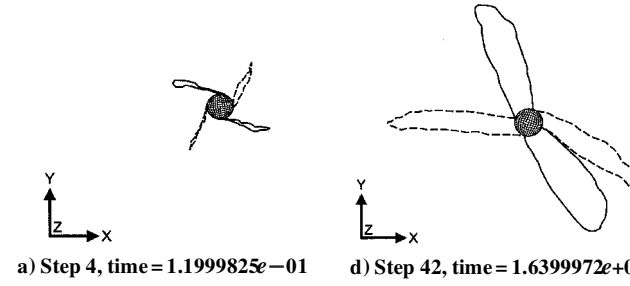

a) Step 4, time = 1.1999825*e*−01 d) Step 42, time = 1.6399972*e*+00

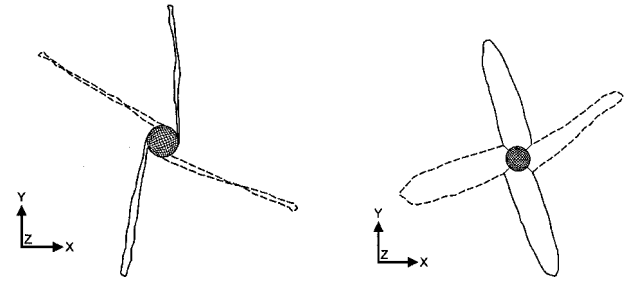

b) Step 10, time = 3.5999849*e*−01 e) Step 55, time = 2.1599975*e*+00

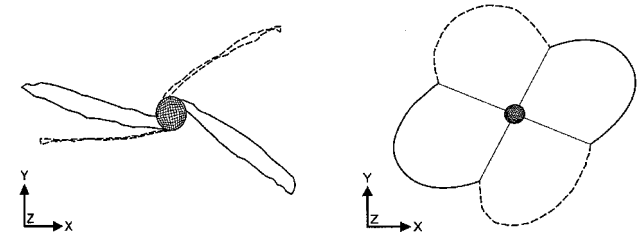

c) Step 18, time = 6.7999804*e*−01 f) Step 94, time = 3.7199931*e*+00

Fig. 14 Effect of random variations in tether damping on deployment stability.

the penetrating nodes. The magnitude of such forces is proportional to the depth of penetration. Results of the deployment analysis are summarized next for a few cases.

In the nominal case, the tether properties described earlier were used. Figure 12 shows a succession of snapshots of the tethers as they unfurled from the packaged state of Fig. 11 to full deployment. Notice the pendulumlike (leading and lagging) motion of the tethers relative to the central rigid cylinder (captured in Figs. 12b and 12c). The frequency of this pendulumlike motion is a function of the tether characteristics and the rate of angular velocity. In the present case, the motion was damped out by the assumed 5% damping, and the deployment proceeded without entanglement. Figures 12e and 12f compare very well to similar instants in the test results shown in Figs. 3 and 4.

The results of the analysis of spin-up rate follow. In the nominal case, a rather fast angular velocity ramp-up time $\Delta t = 0.001$ s was used (a step function). In Fig. 13, we compare the response-time history of a point on the outer edge of the tether between the nominal case (Fig. 13a) and a more gradual spin-up, $\omega_0(t)$, in which $\Delta t = 2$ s was used (Fig. 13b). With the slow spin-up initiation rate (Fig. 13b), excitation of the pendulumlike motion is no longer evident. The growth in response amplitude from 2.0 to 4.4 s is due to the tether radial release.

The results of the analysis of the effect of random variations in properties are now described. The influence of random variability in the tether properties and geometry on their dynamics was studied in this example. Damping was allowed to vary randomly among the four tether segments to within $\pm 20\%$ of the nominal 5% critical damping. The selection of damping as the single random variable was made as a simplification of the more practical but complex scenario, in which random variations could arise from various sources such as changes in properties, length, mass, and cross-sectional area, as well as damping. As can be seen from the sequence of tether motions in Fig. 14, deployment did continue with somewhat chaotic pendulumlike motion of the four tether segments. Especially with longer tethers, it is possible that such variability could have destabilizing effects, eventually resulting in irrecoverable entanglements.

Conclusions

The experiments and simulations described herein were not intended as tools from which one may infer the performance of a real sail in space. Rather, they were intended to provide hands-on experience with the extremely fragile sail film, as well as a basic understanding of some challenging aspects of the spin-deployment dynamics. However, even in the face of the experiment limitations such as sail size, spin-up rate, and the presence of gravity, both the laboratory tests and tether simulations gave strong indications that the proposed deployment scheme is quite feasible.

Acknowledgments

Funding for this research was provided by the Interstellar and Solar Sail Technology Program at the Jet Propulsion Laboratory. The assistance of C. P. Kuo in designing the experiment setup and discussion with C. Garner are greatly appreciated.

References

[1]McInnes, C. R., *Solar Sailing: Technology Dynamics and Mission Applications*, Springer-Praxis, Chichester, England, U.K., 1999.

[2]Salama, M., McInnes, C. R., and Mulligan, P., "Gossamer Sailcraft Technology," *Gossamer Spacecraft Membrane/Inflatable Structures Technology for Space Applications*, edited by C. H. Jenkins, Vol. 191, Progress in Astronautics and Aeronautics, AIAA, Reston, VA, 2001, Chap. 19, pp. 481–501.

[3]Melinov, M. V., and Koshelev, V. A., *Large Space Structures Formed by Centrifugal Forces*, Earth Space Inst. Ser., Gordon and Breach, New York, 1998.

[4]Leipold, M., "ODISSEE—A Proposal for Demonstration of a Solar Sail in Eart Orbit," 3rd International Academy of Astronautics Conf. on Low Cost Planetary Missions, Paper IAA-L98-1005, April 1998.

[5]"The Interstellar Probe Mission Architecture and Technology Report," Jet Propulsion Lab., Rept. JPL-D-18410, California Inst. of Technology, Pasadena, CA, Oct. 1999.

[6]Hallquist, J. O., "LS-DYNA3D Theoretical Manual," Livermore Software Technology, Livermore, CA, 1993.

J. Lassiter
Guest Editor